

# Synthesis, Characterization, Analytical Application, and Theoretical Studies of a Schiff Base, (E)-2-(2-aminophenylthio)-N-(thiophen-2-yl-methylene) benzenamine

**Asnake Lealem Berhanu**

Wollega University

**Irshad Mohiuddin**

Punjabi University

**Ashok Kumar Malik** (✉ [malik\\_chem2002@yahoo.co.uk](mailto:malik_chem2002@yahoo.co.uk))

Punjabi University

**Jatinder Singh Aulakh**

Punjabi University

---

## Research Article

**Keywords:** DFT calculation, detection limit, fluorescence enhancement, mercury (II), Schiff base

**Posted Date:** October 10th, 2022

**DOI:** <https://doi.org/10.21203/rs.3.rs-2124009/v1>

**License:**   This work is licensed under a Creative Commons Attribution 4.0 International License.

[Read Full License](#)

---

**Version of Record:** A version of this preprint was published at Journal of Fluorescence on September 14th, 2023. See the published version at <https://doi.org/10.1007/s10895-023-03435-5>.

# Abstract

In this study, a new Schiff base, (*E*)-2-(2-aminophenylthio)-*N*-(thiophen-2-yl-methylene) benzenamine was synthesized for selective detection of  $\text{Hg}^{2+}$ . This Schiff base was characterized by proton nuclear magnetic resonance ( $^1\text{HNMR}$ ) spectroscopy, carbon-13 nuclear magnetic resonance ( $^{13}\text{CNMR}$ ) spectroscopy, and Fourier-transform infrared (FTIR) spectroscopy. Binding interaction between (*E*)-2-(2-aminophenylthio)-*N*-(thiophen-2-yl-methylene)benzenamine and various metal ions has been studied by UV–Vis spectroscopic measurements and shows promising coordination towards  $\text{Hg}^{2+}$  and almost no interference from other metal ions ( $\text{Ag}^+$ ,  $\text{Mn}^{2+}$ ,  $\text{Fe}^{3+}$ ,  $\text{Al}^{3+}$ ,  $\text{Co}^{2+}$ ,  $\text{Ni}^{2+}$ ,  $\text{Cu}^{2+}$ ,  $\text{Zn}^{2+}$ ,  $\text{Cd}^{2+}$ ,  $\text{Fe}^{2+}$  and  $\text{Cr}^{3+}$ ). This Schiff base exhibiting detection limit of  $3.8 \times 10^{-8}$  M. The Schiff base newly synthesized in this study was successfully applied to the determination of  $\text{Hg}^{2+}$  in water samples. In addition to the experimental study, a theoretical study was conducted using Gaussian 09 program to support the experimental findings. FTIR, NMR, bond angle, bond length, torsional angles and structural approximation were studied using theoretical consideration.

## 1. Introduction

Mercury is widespread in the environment as a result of disposal of industrial and agricultural waste. Its concentration is continuously increasing in the environment due to its extensive industrial applications [1, 2]. Mercury is one of the most hazardous metal ions which can cause substantial damage to human beings even at low concentrations due to its long residence, bioaccumulation and permanent deterioration in the endocrine and central nervous systems, prion and alzheimer's diseases vasodilatation, irritability, paralysis, blindness, result in hearing loss, mental deterioration, speech difficulty, impaired vision, vestibular dysfunction and autism, affect liver and bones upon accumulation in the body, affect stomach, and genes, can causes chromosome breakage, and birth defects, even death [3–5]. It can exist in ionic ( $\text{Hg}^{2+}$ ), elemental ( $\text{Hg}^0$ ), and organic ( $\text{CH}_3\text{Hg}^+$ ) forms. Mercuric ion ( $\text{Hg}^{2+}$ ), more common than mercurous ion ( $\text{Hg}^+$ ), is a caustic and carcinogenic material with high cellular toxicity. Especially inorganic  $\text{Hg}^{2+}$  is a serious pollutant; thus, it must be removed properly from natural water and wastewater effluents.

The determination of trace amounts of heavy metal ions (such as  $\text{Hg}^{2+}$ ) is of interest in many fields including environmental analysis, process control, biology, and medicine. The growing awareness of environmental mercury pollution and toxicity necessitates its determination, even at very low concentrations in water. For drinking water, the allowed mercury level is  $1 \mu\text{gL}^{-1}$ , set by World Health Organization (WHO) [6, 7].

Transition metal complexes containing Schiff base ligands have been a subject of specific interest in synthetic chemistry [8]. Even though many methods have already been developed to detect  $\text{Hg}^{2+}$ , there is still a need to develop more sensitive, selective, and simple way to detect the mercury ion existing in environmental samples. Fluorescence detection is more advantageous than other techniques due to its

high sensitivity, applicability to field investigation, and low cost [9–11]. In this study, a Schiff base containing nitrogen and sulphur was developed as a sensor having a low detection limit for  $\text{Hg}^{2+}$  in water.

To the best of the authors' knowledge, no prior studies have estimated theoretical and experimental values by using (*E*)-2-(2-aminophenylthio)-*N*-(thiophen-2-yl-methylene) benzenamine for fluorescence detection of  $\text{Hg}^{2+}$  in different water samples. In this regard, a detailed theoretical and experimental investigations into the vibrational spectra and thermodynamic data of the molecule was conducted.

## 2. Materials And Methods

### 2.1. Synthesis of the Schiff base, (*E*)-2-(2-aminophenylthio)-*N*-(thiophen-2-yl-methylene) benzenamine

Reagents and chemicals were obtained from Avra Synthesis (Hyderabad India) and TCI Chemicals (Chennai India). They were used without further purification. A 20 mL ethanol solution of 2-(2-aminophenyl)sulfide (5 mM, 1.082 g) was mixed on stirring with a 20 mL ethanol solution of thiophene-2-carbaldehyde (5 mM, 0.468 g), followed by being refluxed at 60°C for 8 h. After cooling in the deep freezing for 2 days the yellow product was collected washed with ethanol and dried in desiccator over  $\text{CaCl}_2$ . Scheme 1 describes the procedure of synthesizing the Schiff base.

### 2.2. Characterization and theoretical study of the Schiff base

Completion of the reaction was checked by using thin layer chromatography (TLC). Proton nuclear magnetic resonance ( $^1\text{H}$ NMR) and carbon-13 nuclear magnetic resonance ( $^{13}\text{C}$ NMR) spectra were obtained by using a BRUKER AVACE II 400 MHz NMR spectrometer. For the Fourier transform infrared (FTIR) analysis, a Perkin Elmer 100 FTIR spectrometer was used. A Shimadzu UV-1800 spectrophotometer was employed to obtain UV-Vis spectra. Fluorescence of the sample was recorded using a Shimadzu RF 5301PC Spectrofluorophotometer. The theoretical studies were carried out using Gaussian 09 software.

### 2.3. Preparation of real water samples

Three water samples were collected from different areas: tube well water from Mehmoodpur Araian, drinking water and tap water from Chemistry Department Punjabi University, Patiala (India). Prior to any experiment, the tube well water was centrifuged to remove the impurities such as sands. Before doing any further sample pre-treatment, all the collected ground water samples were investigated by the synthesised probe for  $\text{Hg}^{2+}$  presence, so as to show the applicability of the reported probe under real world conditions. However,  $\text{Hg}^{2+}$  was not detected or was below the method detection limit in the ground water samples. The water samples were spiked with different concentrations of  $\text{Hg}^{2+}$ . From each 10.0 mL of water sample were taken and diluted with buffer of pH = 8.0 solution in a 25 mL volumetric flask. Different

amount of (0, 5, 10, 15, 20, 30, 40, 50 mL) 10  $\mu\text{M}$   $\text{Hg}^{2+}$  standard solution was added and filled to the mark. From the calibration curve of spike vs volume of standard added concentration of  $\text{Hg}^{2+}$  ions in water samples were calculated.

## 3. Results And Discussion

### 3.1. Experimental study

#### 3.1.1. $^1\text{H}$ NMR and $^{13}\text{C}$ NMR analysis

$^1\text{H}$ NMR of the (*E*)-2-(2-aminophenylthio)-*N*-(thiophen-2-yl-methylene) benzenamine taken at the conditions (400 MHz, dimethyl sulfoxide ( $\text{DMSO-d}_6$ ) solvent,  $\delta$  in ppm) showed a chemical shift at 5.39 (s, 2H of  $\text{NH}_2$ ), 6.5814–7.0798 (m, 8H, of Aromatic), 7.3202–7.8765 (m, 3H, of thiophene), and 8.77 (d, 1H of  $\text{CH} = \text{N}$ ). The presence of 14 protons at different chemical shifts indicated the formation of the Schiff base as expected. The absence of picks at around 9.0–10.0 ppm indicated that aldehyde hydrogen is replaced, instead of azomethine hydrogen appeared at 8.77 ppm. Figures S1 and S2 shows  $^1\text{H}$ NMR and  $^{13}\text{C}$ NMR spectrum of the Schiff base, respectively.

$^{13}\text{C}$  NMR analysis also confirmed the formation of the ligand, indicating the number of carbon atoms present at correspond chemical shifts. There were 17 carbons in the ligands. Different carbons appeared at different chemical shifts. Each carbon was indicated as follows: (C-8, 111  $\delta$ ), (C-12, 114  $\delta$ ), (C-1, 116  $\delta$ ), (C-10, 118  $\delta$ ), (C-17, 125.25  $\delta$ ), (C-3, 125.79  $\delta$ ), (C-16, 126  $\delta$ ), (C-4, 128  $\delta$ ), (C-18, 131.07  $\delta$ ), (C-11, 131.75  $\delta$ ), (C-5, 132  $\delta$ ), (C-9, 133  $\delta$ ), (C-2, 137  $\delta$ ), (C-19, 142  $\delta$ ), (C-13, 147  $\delta$ ), (C-21, 150  $\delta$ ), and (C-6, 153  $\delta$ ).

#### 3.1.2. FTIR analysis of the ligands

From the FTIR spectrum of the ligand (Figure S3) at 3441 and 3326  $\text{cm}^{-1}$  for N-H stretching, 3055  $\text{cm}^{-1}$  for stretching of  $\text{sp}^2$  hybrid C-H, 1607  $\text{cm}^{-1}$  for  $\text{N} = \text{C}$  stretching, 1462  $\text{cm}^{-1}$  for aromatic C-C stretching, and 713  $\text{cm}^{-1}$  for C-S-C stretching. The results indicated the formation of azomethine bond.

#### 3.1.3. Electronic spectroscopy analysis results

The UV–Vis spectra of the Schiff base were examined in the range of 200–800 nm in six organic solvent systems such as ethanol, methanol, DMSO, *N,N*-dimethylformamide (DMF), DMF/ $\text{H}_2\text{O}$ , and acetonitrile/ $\text{H}_2\text{O}$ . Among these solvent systems, DMF/ $\text{H}_2\text{O}$  gave the best results, thereby being chosen for further spectroscopic studies. The UV–Vis spectra are shown in Fig. 1. The maximum absorptions observed in the range from 320 to 250 nm were attributed to  $\pi\check{\pi}^*$  transitions of  $\pi$  electrons within the structure. Absorption intensity of  $\pi\check{\pi}^*$  transitions decreased in an order: DMF/ $\text{H}_2\text{O}$  > DMSO >  $\text{CH}_3\text{CN}$  > ethanol > methanol > acetonitrile/ $\text{H}_2\text{O}$  (hyper chromic effect). The absorption intensity at 220 nm belonged to  $n\check{\pi}^*$  transitions was observed in the DMF/ $\text{H}_2\text{O}$  system. Absorption spectra for the complexes were also recorded in the DMF/ $\text{H}_2\text{O}$  solution. In the spectra of the complexes,  $\pi\check{\pi}^*$  and  $n\check{\pi}^*$

transitions observed in the ligand was not affected by any kind of metal ions. The absorption at 280nm shifted to 320 nm by complexing with  $\text{Hg}^{2+}$  (bathochromic shift), indicating chelation of the Schiff base with  $\text{Hg}^{2+}$  ions. To further confirm sensitivity of the Schiff base to  $\text{Hg}^{2+}$ , fluorescence studies were conducted.

### 3.1.4. Quantum yield

The fluorescence quantum yield ( $\Phi$ ) of Schiff base was noted as 0.21 in ethanol by taking anthracene as standard. The fluorescence excitation (310–365 nm) and fluorescence emission wavelength (370–450 nm) of anthracene corroborated with the excitation (310 nm) and emission wavelength (440 nm) of Schiff base. Anthracene displayed quantum yield of 0.27 in the ethanol.

### 3.1.5. Fluorescence spectral studies of the Schiff base and its metal complexes

The fluorescence spectra of the (*E*)-2-(2-aminophenylthio)-*N*-(thiophen-2-yl-methylene) benzenamine ( $1 \times 10^{-5}$  M) obtained in the DMF / $\text{H}_2\text{O}$  (7:3 v/v; pH = 8.0) system with metal ions such as  $\text{Ag}^+$ ,  $\text{Mn}^{2+}$ ,  $\text{Fe}^{3+}$ ,  $\text{Al}^{3+}$ ,  $\text{Co}^{2+}$ ,  $\text{Ni}^{2+}$ ,  $\text{Cu}^{2+}$ ,  $\text{Zn}^{2+}$ ,  $\text{Cd}^{2+}$ ,  $\text{Hg}^{2+}$ ,  $\text{Fe}^{2+}$ , and  $\text{Cr}^{3+}$  (1.0 equiv.) are shown in Fig. 2. In free state, it was displayed a weak fluorescence emission band at 440 nm up on excitation at 310 nm. The emission intensity at 440 nm was increased with an addition of  $\text{Hg}^{2+}$ , attributed to strong interactions between the Schiff base and  $\text{Hg}^{2+}$ . However, no significant variation in the emission intensity was observed with additions of other metal cations. The high selectivity toward  $\text{Hg}^{2+}$  was likely due to a compatible ion size and a high binding affinity between the metal ions and the Schiff base. Therefore, the (*E*)-2-(2-aminophenylthio)-*N*-(thiophen-2-yl-methylene)benzenamine could serve as a highly selective “turn-on” fluorescent chemosensor for  $\text{Hg}^{2+}$ .

### 3.1.6. Fluorescence titrations of the Schiff base with $\text{Hg}^{2+}$

As shown in Fig. 3, an increase in fluorescence intensity was observed in the DMF/ $\text{H}_2\text{O}$  (7:3 v/v) solution with increasing  $\text{Hg}^{2+}$  concentration from 0.1 to 1.0 equi. The maximum concentration was 1.0 equi. of  $1 \times 10^{-5}$  M  $\text{Hg}^{2+}$ .

### 3.1.7. Determination of limit of detection and comparison with literature values

Limit of detection (LOD) of a fluorescence sensor was determined as shown in Fig. 4 which illustrates a plot of emission intensity vs. concentration of  $\text{Hg}^{2+}$  ( $\text{LOD} = 3\sigma/k$ , where  $\sigma$  standard deviation of the blank,  $k$  is slope and found to be  $3.8 \times 10^{-8}$  M). The detection limit of the sensor developed in this study was compared to previously reported values (Table 1). According to the comparison (Table 1), the (*E*)-2-(2-aminophenylthio)-*N*-(thiophen-2-yl-methylene) benzenamine was effective to detect  $\text{Hg}^{2+}$  with a lower detection limit.

Table 1

The comparison LOD of (*E*)-2-(2-aminophenylthio)-*N*-(thiophen-2-yl-methylene) benzenamine with other Schiff bases reported in previous literature.

| Order | Schiff bases  | Signal                        | LOD(M)                 | References |
|-------|---|-------------------------------|------------------------|------------|
| 1     | 2-(Benzothiazol-2-yliminomethyl)-4-nitrophenol,   | Colorimetric                  | $1.5 \times 10^{-7}$   | [1]        |
| 2     | 2-(Pyridin-2-yl)benzothiazole   | Fluorescent                   | $15 \times 10^{-6}$    | [18]       |
| 3     | ( <sup>2</sup> E, <sup>2'</sup> E)-2,2'-(4,4'-(Acenaphtho[1,2-b]quinoxaline-8,11-diyl)bis(4,1-phenylene))bis(methan-1-yl-1-ylidene)bis(hydrazine carbo thioamide) | Fluorescent                   | $9.07 \times 10^{-7}$  | [4]        |
| 4     | 2-((E)-((E)-3-(4-(Dimethyl amino)phenyl)allylidene) amino)-2-phenyl ethanol   | Fluorescence and calorimetric | $3.15 \times 10^{-6}$  | [5]        |
| 5     | <i>N,N</i> -Dimethyl-4-[( <sup>1</sup> E, <sup>3</sup> E)-3-{2-[4-(trifluoromethyl)pyrimidin-2-yl] hydrazinylidene}prop-1-en-1-yl]aniline                         | Colorimetric                  | $3.9 \times 10^{-7}$   | [19]       |
| 6     | (E)-8-((2-( <sup>1</sup> H-Benzo[d]imidazol-2-yl)phenylimino) methyl)-7-hydroxy-4-methyl-2H-chromen-2-one   | Fluorescent and colorimetric  | $1.202 \times 10^{-7}$ | [20]       |
| 7     | ( <i>E</i> )-2-(2-Aminophenylthio)- <i>N</i> -(thiophen-2-yl-methylene) benzenamine   | Fluorescence                  | $3.8 \times 10^{-8}$   | This- work |

### 3.1.8. Determination of binding constant

Binding constant was calculated based on the fluorescence intensity data using the Benesi Hildebrand equation [12]. Figure 5 shows linear relationship between  $(F_{\max} - F_{\min}) / (F - F_{\min})$  at 640 nm and  $1/[Hg^{2+}]$ . The binding constant of the complex of the (*E*)-2-(2-aminophenylthio)-*N*-(thiophen-2-yl-methylene) benzenamine and  $Hg^{2+}$  was calculated as  $1.5 \times 10^4 M^{-1}$ .

### 3.1.9. Determination of stoichiometry of the complex

To identify stoichiometry between the (*E*)-2-(2-aminophenylthio)-*N*-(thiophen-2-yl-methylene) benzenamine and  $Hg^{2+}$ , the fluorescence behavior was studied by using the Job's method (Fig. 6). Their total concentrations were kept constant, and mole fraction of  $Hg^{2+}$  was varied from 0 to 1.0. The maximum intensity was achieved when the molar fraction of  $Hg^{2+}$  reached 0.5, indicating the stoichiometry of the (*E*)-2-(2-aminophenylthio)-*N*-(thiophen-2-yl-methylene) benzenamine to  $Hg^{2+}$  be 1:1.

### 3.1.10. Selectivity study

Selectivity was assessed through competitive experiments. The changes in fluorescence of the Schiff base in the DMF/H<sub>2</sub>O (7:3 v/v) solution were measured by the treatment of Hg<sup>2+</sup> (1.0 equiv.) in the presence of other interfering metal cations such as Ag<sup>+</sup>, Mn<sup>2+</sup>, Fe<sup>3+</sup>, Al<sup>3+</sup>, Co<sup>2+</sup>, Ni<sup>2+</sup>, Cu<sup>2+</sup>, Zn<sup>2+</sup>, Cd<sup>2+</sup>, Fe<sup>2+</sup>, and Cr<sup>3+</sup> (1.0 equiv.) (Fig. 7). No obvious change in fluorescence was observed regardless of existence of other cations. Relative error (%) was calculated using the relation: Relative error % = ( $\Delta F/F_0 \times 100\%$ ) [13], where  $\Delta F$  is the difference of fluorescence intensities before and after exposure to interferent cations. Note that the relative error less than  $\pm 5\%$  can be acceptable. The value of the relative error listed in Table 2, showing that the Schiff base had a high selectivity to Hg<sup>2+</sup> despite the existence of the interferent ions.

Table 2  
Effect of interferent cations on the fluorescence signal of the optical sensor.

| Order | Interferent      | Relative error % |
|-------|------------------|------------------|
| 1     | Mn <sup>2+</sup> | 1.05             |
| 2     | Al <sup>3+</sup> | 1.11             |
| 3     | Fe <sup>3+</sup> | 1.15             |
| 4     | Fe <sup>2+</sup> | 1.18             |
| 5     | Cd <sup>2+</sup> | 1.25             |
| 6     | Ni <sup>2+</sup> | 1.19             |
| 7     | Zn <sup>2+</sup> | 1.85             |
| 8     | Cu <sup>2+</sup> | 1.92             |
| 9     | Co <sup>2+</sup> | 1.27             |
| 10    | Cr <sup>3+</sup> | 2.70             |
| 11    | Ag <sup>+</sup>  | 3.25             |

### 3.1.11. Effect of pH and solvent

Without Hg<sup>2+</sup>, the weak fluorescence intensity of the Schiff base solution could be observed from pH 1.0 to 12. With an addition of Hg<sup>2+</sup> (1.0 equiv.), the fluorescence intensity was increased from 100 to 900 a.u. with an increase in pH from 6 to 8. A further increase in pH from 8 to 12 decreased the fluorescence intensity to 100 a.u. (Figure S4). It was attributed to the Schiff base binding Hg<sup>2+</sup> prevented at low pH value. At high pH values, weak fluorescence was presented. In addition, as showed in Figure S5, the

optimum fluorescence enhancement occurred in the presence of the DMF/H<sub>2</sub>O solvent. Therefore, pH = 8.0 and the DMF/H<sub>2</sub>O solvent were selected for further studies.

## 3.2. Theoretical study

In this section, computational data of the (*E*)-2-(2-aminophenylthio)-*N*-(thiophen-2-yl-methylene) benzenamine were compared with the experimental results discussed in section 3.1. Energy of the lowest unoccupied molecular orbitals ( $E_{\text{LUMO}}$ ) indicates the tendency of a molecule to accept electrons from donor molecules. The lower this energy, the better the chance to accept electrons. A larger difference in energy between the highest occupied molecular orbitals (HOMO) and lowest unoccupied molecular orbital (LUMO) means a higher stability of molecules and complexes. Hardness ( $\chi$ ) is the measure of resistance to charge transfer. This property can be calculated from half of the difference between  $E_{\text{HOMO}}$  and  $E_{\text{LUMO}}$ . Chemical softness ( $S$ ) is the capacity of an atom or group of atoms to receive electrons, which is half of the hardness ( $\chi$ ) [14, 15]. The binding energy between the metal cation and ligands can be calculated using the following relation [16]:

$$\Delta E = E_{\text{complex}} - (E_{\text{cation}} + E_{\text{ligand}})$$

where  $\Delta E$  is the change in energy;  $E_{\text{complex}}$  is the total energy of the complex;  $E_{\text{cation}}$  is energy of cation; and  $E_{\text{ligand}}$  is energy of the ligand. All the investigated parameters of theoretical studies including vibrational analysis, NMR spectra, thermodynamic parameters, Mulliken charge distribution, natural bond orbital analysis, natural electron configuration are presented in the Section S1 of supplementary information.

### 3.2.1. Geometrical optimization and Frontier molecular orbitals (FMO)

The optimized geometries of Schiff base and Schiff base complex with Hg were obtained by using a basis set of LANL2DZ/B3LYP are shown in Fig. 8. Frontier molecular orbitals (FMO), HOMO, and LUMO play an important role in quantum chemistry. The FMO theory is useful to predict relative reactivity based on properties of the reactants [17]. The difference in energy between FMO of the (*E*)-2-(2-aminophenylthio)-*N*-(thiophen-2-yl-methylene) benzenamine was calculated, and the results are shown in Fig. 9a ( $E_{\text{HOMO}} = -0.198$  a.u. and  $E_{\text{LUMO}} = -0.067$  a.u.; the change calculated as:  $\Delta E = \text{HOMO-LUMO}$ ,  $-0.198 - (-0.0671)$  a.u. =  $-0.130$  a.u.;  $\chi = 1/2(\text{HOMO-LUMO}) = 1/2(0.130) = 0.065$  a.u.,  $S = 1/2(\chi) = 1/2(0.065) = 0.0325$  a.u.). When the Schiff base was complexed with Hg<sup>2+</sup>, the energy of the complex became lower (Fig. 9b). The energy for free (*E*)-2-(2-aminophenylthio)-*N*-(thiophen-2-yl-methylene) benzeneamine was found to be  $-1561$  hartree while that of the complex with Hg<sup>2+</sup> was  $-1615$  hartree. The calculated change in energy of the Hg<sup>2+</sup> complex was  $-12.58$  hartree using following equation:

$$\Delta E = E_{\text{complex}} - (E_{\text{cation}} + E_{\text{ligand}}) = -1615 - (-41.42 + (-1561)) = -12.58 \text{ hartree}$$



By using the same basis set energy of different metal complexes of (*E*)-2-(2-aminophenylthio)-*N*-(thiophen-2-yl-methylene) benzenamine were studied and compared for the relative stability. The smallest energy was obtained for the complex between the Schiff base and  $\text{Hg}^{2+}$ . This result indicated that the Schiff base forms more stable complexes with  $\text{Hg}^{2+}$  than the other metal ions tested in this study. This agreed with the fluorescence study for the selectivity of the Schiff base.

### **3.3. Application to real water samples**

To verify practical application of the Schiff base, standard solution of  $\text{Hg}^{2+}$  was spiked to real water samples (e.g., tap water, drinking water, and tub well water) and fluorescence was monitored in situ to quantitatively detect  $\text{Hg}^{2+}$  ions in the samples. Table 3 shows the experimental results obtained using the real water samples. The recoveries of the real water samples were in the range from 98 to 104% with relative standard deviations (%RSDs) varied from 1.3 to 2.8%. The results showed that the developed optical sensor (i.e., the Schiff base) for  $\text{Hg}^{2+}$  is effective to detect mercury ion in real water, and the proposed mercury detection method may have great potential for applications to monitoring of mercury contained in water in nature.

Table 3

Determination of  $\text{Hg}^{2+}$  in different water samples from different sources by a standard addition method.

| Matrixes        | Amount of standard added (n = 3) ( $\mu\text{M}$ ) | Total amount Found (n = 3) ( $\mu\text{M}$ ) | % Recovery | %RSD | Correlation coefficient ( $R^2$ ) |
|-----------------|--|--|------------|------|-----------------------------------|
| Tap water       | 0  | 0  | -          | -    | 0.9991                            |
|                 | 20   | 20.8   | 104        | 2.8  |                                   |
|                 | 30   | 30.5   | 101        | 1.6  |                                   |
|                 | 40   | 39.2   | 98         | 2.0  |                                   |
| Drinking water  | 0  | 0  |            |      | 0.9997                            |
|                 | 20   | 20.3   | 101        | 2.8  |                                   |
|                 | 30   | 30.7   | 102        | 1.3  |                                   |
|                 | 40   | 40.3   | 100        | 1.3  |                                   |
| Tube well water | 0  | 0  |            |      | 0.9994                            |
|                 | 20   | 20.9   | 104        | 2.2  |                                   |
|                 | 30   | 30.8   | 102        | 1.6  |                                   |
|                 | 40   | 39.6   | 99         | 1.5  |                                   |

## 4. Conclusions

Herein, it was developed a fluorescence probe Schiff base, (*E*)-2-(2-aminophenylthio)-*N*-(thiophen-2-yl-methylene)benzenamine. The Schiff base effectively detected  $\text{Hg}^{2+}$  in different water samples such as tap water, drinking water, and tube well water. The method using the Schiff base was validated by recovery study, interference study, and relative standard deviation study. The Schiff base was also effective to detect  $\text{Hg}^{2+}$  in the presence of competing cations (e.g.,  $\text{Ag}^+$ ,  $\text{Mn}^{2+}$ ,  $\text{Fe}^{3+}$ ,  $\text{Al}^{3+}$ ,  $\text{Co}^{2+}$ ,  $\text{Ni}^{2+}$ ,  $\text{Cu}^{2+}$ ,  $\text{Zn}^{2+}$ ,  $\text{Cd}^{2+}$ ,  $\text{Hg}^{2+}$ ,  $\text{Fe}^{2+}$  and  $\text{Cr}^{3+}$ ). The Schiff base, (*E*)-2-(2-aminophenylthio)-*N*-(thiophen-2-yl-methylene)benzenamine, exhibited a detection limit of  $3.8 \times 10^{-8}$  M with a binding constant of be  $1.5 \times 10^4$   $\text{M}^{-1}$ , which is lower than the detection limit of typical  $\text{Hg}^{2+}$  detection methods. The experimental findings were supported by theoretical studies. In the theoretical part, different metals were simulated to investigate the metal complexes based on their stability. To identify what kind of complexes of the Schiff base is stable, the structure of different metals were optimized. Based on the theoretical study results, it could be

concluded that the Schiff base, (*E*)-2-(2-aminophenylthio)-*N*-(thiophen-2-yl-methylene) benzenamine, selectively forms a stable complex with Hg<sup>2+</sup> than the other metal ions tested in this study. The results of recovery study indicated that the Schiff base is effective for the detection of Hg<sup>2+</sup>. The proposed detection method may have great potential for the application to monitoring mercury ion in real environmental samples.

## Declarations

### Acknowledgements

The authors thank the Department of Chemistry, Punjabi University, Patiala, India and the Federal Democratic Republic of Ethiopia for their support. The authors are also highly thankful to Prof. Ki-Hyun Kim (Hanyang University, Seoul, Republic of Korea) and Dr. Jechan Lee (Ajou University, Suwon, Republic of Korea) for greatly improving the manuscript.

### Author Declarations

**Funding** The authors thank the Department of Chemistry, Punjabi University, Patiala, India and the Federal Democratic Republic of Ethiopia for their support.

**Conflicts of interest** The authors have no conflicts of interest.

**Availability of data and material** All the data associated with this research has been presented in this paper.

**Code availability** Not applicable.

**Authors' contributions.** **Asnake Lealem:** Conceptualization, Methodology, Data curation, Writing-original draft, Visualization, Validation. **Irshad Mohiuddin:** Methodology, Writing-original draft, Writing-review and editing, Validation. **Ashok Kumar Malik:** Investigation, Methodology, Project Administration, Resources, Software, Supervision, Validation, Visualization, Writing-review and editing. **Jatinder Singh Aulakh:** Project administration, Investigation, Supervision, Writing-review and editing. All authors read and approved the final manuscript.

**Ethics Approval** Not applicable.

**Consent to participate** Not applicable.

**Consent for publication** Not applicable.

## References

1. Momidi, B.K., V. Tekuri, and D.R. Trivedi, *Selective detection of mercury ions using benzothiazole based colorimetric chemosensor*. Inorganic Chemistry Communications, 2016. **74**: p. 1-5.

2. Zeng, H., et al., *Highly efficient and selective removal of mercury ions using hyperbranched polyethylenimine functionalized carboxymethyl chitosan composite adsorbent*. Chemical Engineering Journal, 2019. **358**: p. 253-263.
3. Wang, J., W. Li, and L. Long, *Development of a near-infrared fluorescence turn-on probe for imaging Hg<sup>2+</sup> in living cells and animals*. Sensors and Actuators B: Chemical, 2017. **245**: p. 462-469.
4. Feng, L., et al., *A novel thiosemicarbazone Schiff base derivative with aggregation-induced emission enhancement characteristics and its application in Hg<sup>2+</sup> detection*. Sensors and Actuators B: Chemical, 2016. **237**: p. 563-569.
5. Jiménez-Sánchez, A., N. Farfán, and R. Santillan, *A reversible fluorescent–colorimetric Schiff base sensor for Hg<sup>2+</sup> ion*. Tetrahedron Letters, 2013. **54**(39): p. 5279-5283.
6. Aziz, A.A.A. and S.H. Seda, *Detection of trace amounts of Hg<sup>2+</sup> in different real samples based on immobilization of novel unsymmetrical tetradentate Schiff base within PVC membrane*. Sensors and Actuators B: Chemical, 2014. **197**: p. 155-163.
7. Ismaiel, A.A., M.K. Aroua, and R. Yusoff, *Potentiometric determination of trace amounts of mercury (II) in water sample using a new modified palm shell activated carbon paste electrode based on kryptofix 5*. 2012.
8. Karmakar, D., et al., *Synthesis and crystal structure of a group of phenoxo-bridged heterodinuclear [NiIIHgII] Schiff base complexes*. Polyhedron, 2013. **49**(1): p. 93-99.
9. Xia, N., et al., *The detection of mercury ion using DNA as sensors based on fluorescence resonance energy transfer*. Talanta, 2019. **192**: p. 500-507.
10. Huo, Y., et al., *Highly selective and sensitive colorimetric chemosensors for Hg<sup>2+</sup> based on novel diaminomaleonitrile derivatives*. RSC advances, 2016. **6**(7): p. 5503-5511.
11. Bhogal, S., et al., *Synchronous Fluorescence Determination of Al<sup>3+</sup> Using 3-Hydroxy-2-(4-Methoxy Phenyl)-4H-Chromen-4-One as a Fluorescent Probe*. Journal of Fluorescence, 2022. **32**(1): p. 359-367.
12. Sharma, P., et al., *Experimental and Theoretical Studies of the Pyrazoline Derivative 5-(4-methylphenyl)-3-(5-methylfuran-2-yl)-1-phenyl-4, 5-dihydro-1H-Pyrazole and its Application for Selective Detection of Cd<sup>2+</sup> ion as Fluorescent Sensor*. Journal of Fluorescence, 2022. **32**(3): p. 969-981.
13. Sharma, P., et al., *Fluorescence “Turn-off” Sensing of Iron (III) Ions Utilizing Pyrazoline Based Sensor: Experimental and Computational Study*. Journal of Fluorescence, 2022: p. 1-13.
14. Farhadi, S., F. Mahmoudi, and J. Simpson, *A new nano-scale manganese (II) coordination polymer constructed from semicarbazone Schiff base and dicyanamide ligands: Synthesis, crystal structure and DFT calculations*. Journal of Molecular Structure, 2016. **1108**: p. 583-589.
15. Parsaee, Z., et al., *A novel high performance nano chemosensor for copper (II) ion based on an ultrasound-assisted synthesized diphenylamine-based Schiff base: Design, fabrication and density functional theory calculations*. Ultrasonics Sonochemistry, 2018. **41**: p. 337-349.
16. Pramanik, H.A., et al., *Mixed ligand complexes of cobalt (III) and iron (III) containing N<sub>2</sub>O<sub>2</sub>-chelating Schiff base: Synthesis, characterisation, antimicrobial activity, antioxidant and DFT study*. Journal of

Molecular Structure, 2015. **1100**: p. 496-505.

17. Jensen, F., *Introduction to computational chemistry*. 2017: John Wiley & Sons.

18. Dhaka, G., J. Singh, and N. Kaur, *Benzothiazole based chemosensors having appended amino group (s): Selective binding of Hg<sup>2+</sup> ions by three related receptors*. *Inorganica Chimica Acta*, 2017. **462**: p. 152-157.

19. Jung, J.M., C. Kim, and R.G. Harrison, *A dual sensor selective for Hg<sup>2+</sup> and cysteine detection*. *Sensors and Actuators B: Chemical*, 2018. **255**: p. 2756-2763.

20. Gao, Y., et al., *A fluorescent and colorimetric probe enables simultaneous differential detection of Hg<sup>2+</sup> and Cu<sup>2+</sup> by two different mechanisms*. *Sensors and Actuators B: Chemical*, 2017. **238**: p. 455-461.

## Scheme

Scheme1 is available in the Supplementary Files section.

## Figures

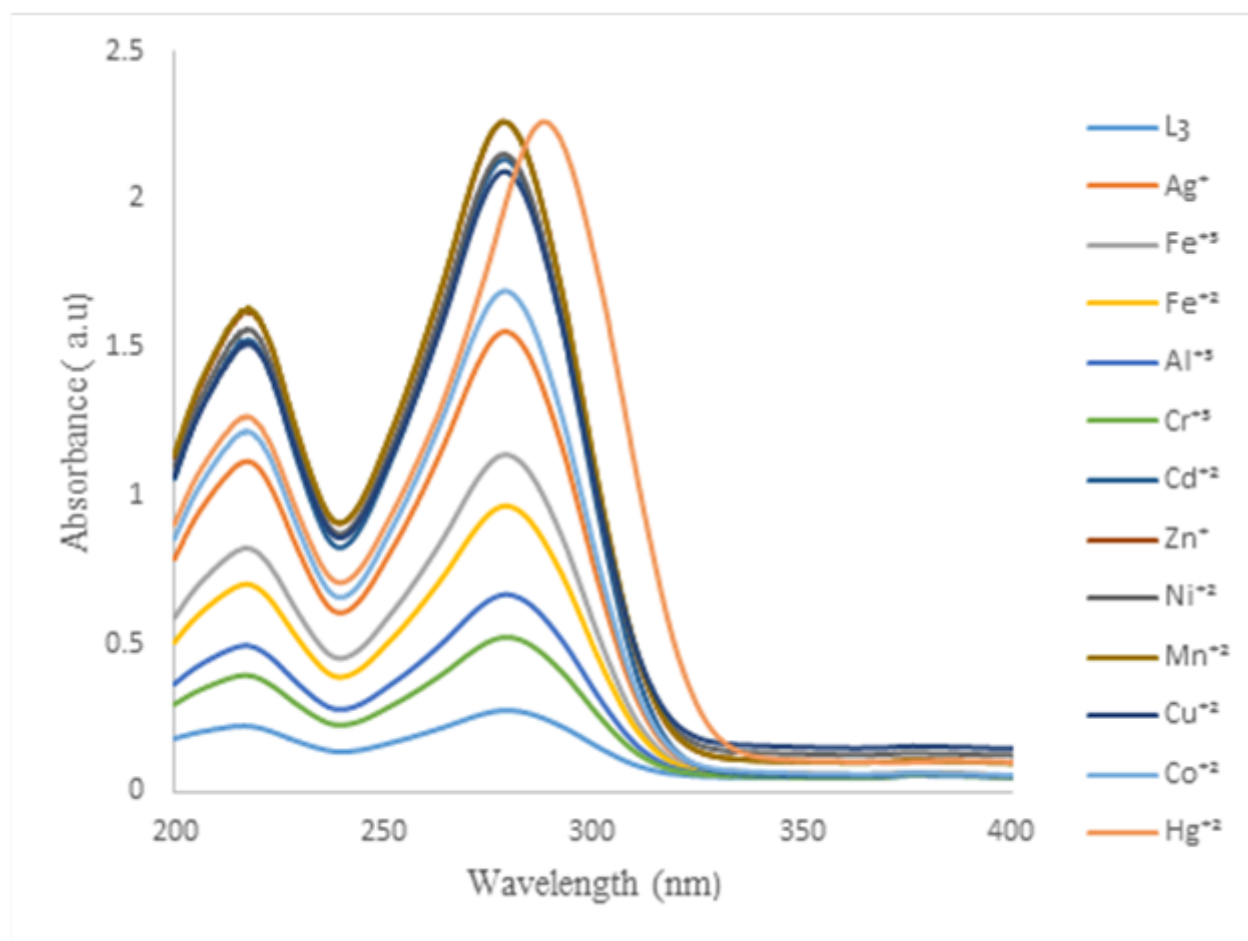


Figure 1

UV spectra of the (*E*)-2-(2-aminophenylthio)-*N*-(thiophen-2-yl-methylene) benzenamine and its metal complexes ( $1 \times 10^{-5}$  M, pH = 8.0)

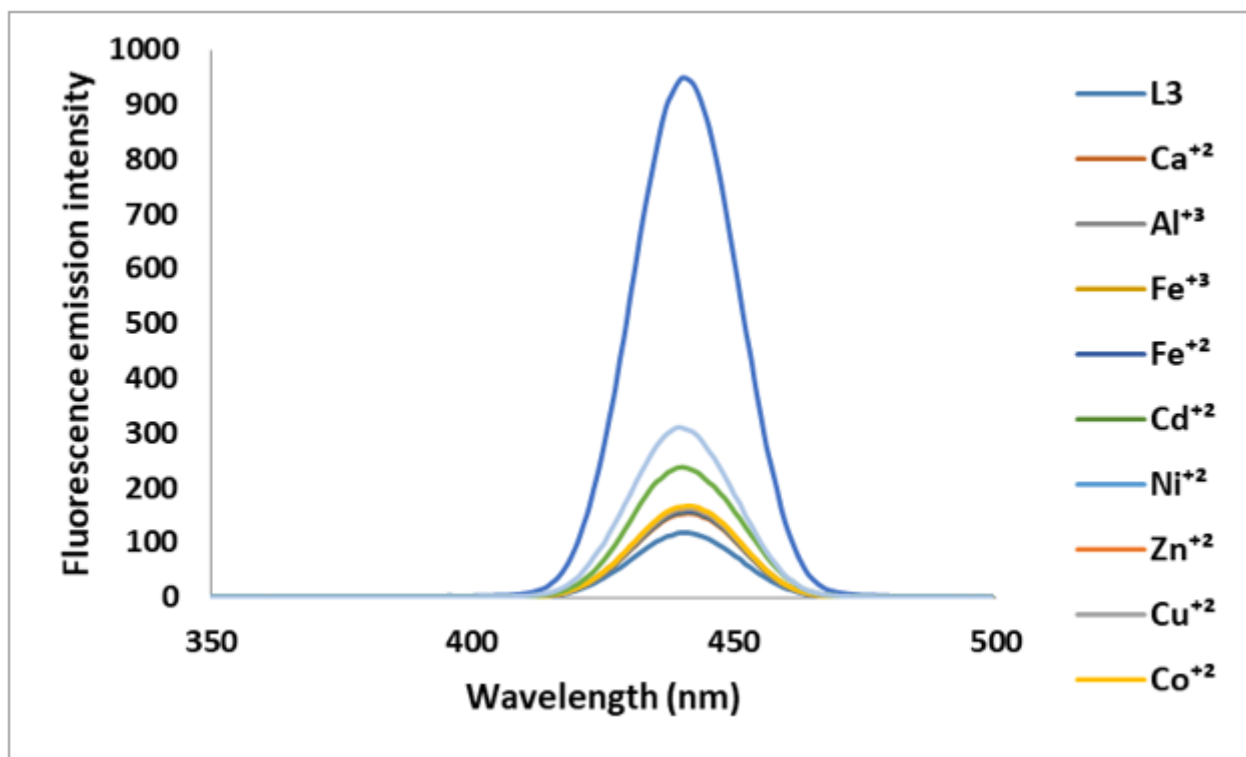


Figure 2

Fluorescence spectra of the (*E*)-2-(2-aminophenylthio)-*N*-(thiophen-2-yl-methylene) benzenamine ( $1 \times 10^{-5}$  M) with Hg<sup>2+</sup> and other metal ions

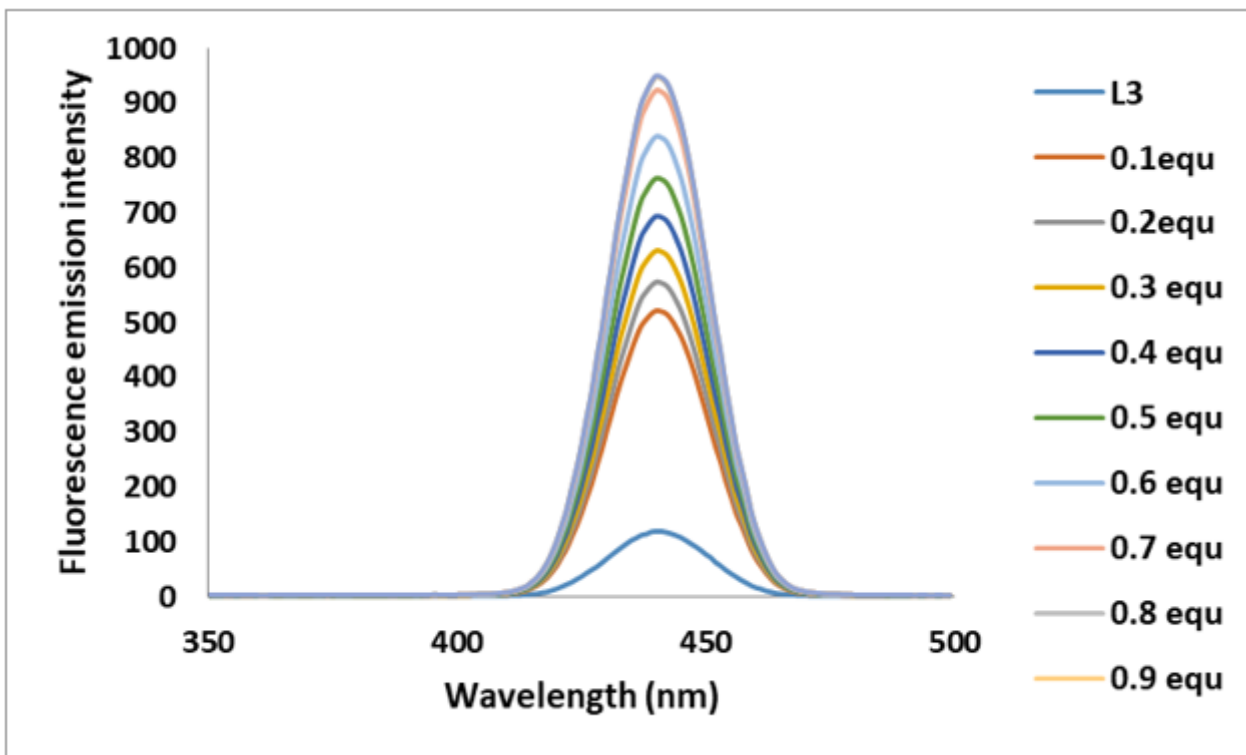


Figure 3

Fluorescence spectra of *(E)*-2-(2-aminophenylthio)-*N*-(thiophen-2-yl-methylene) benzenamine ( $1 \times 10^{-5}$  M) with addition of increasing amount of  $\text{Hg}^{2+}$

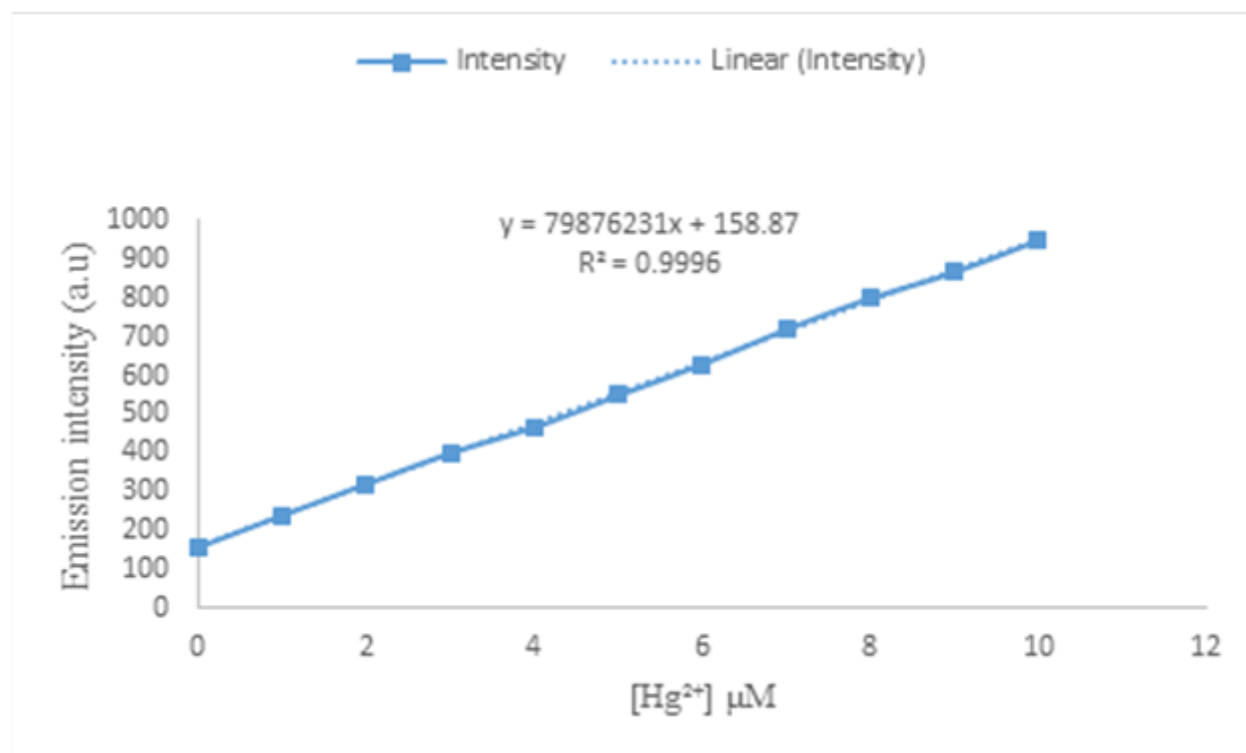


Figure 4

Linear plot of fluorescence emission intensity versus concentration of  $\text{Hg}^{2+}$

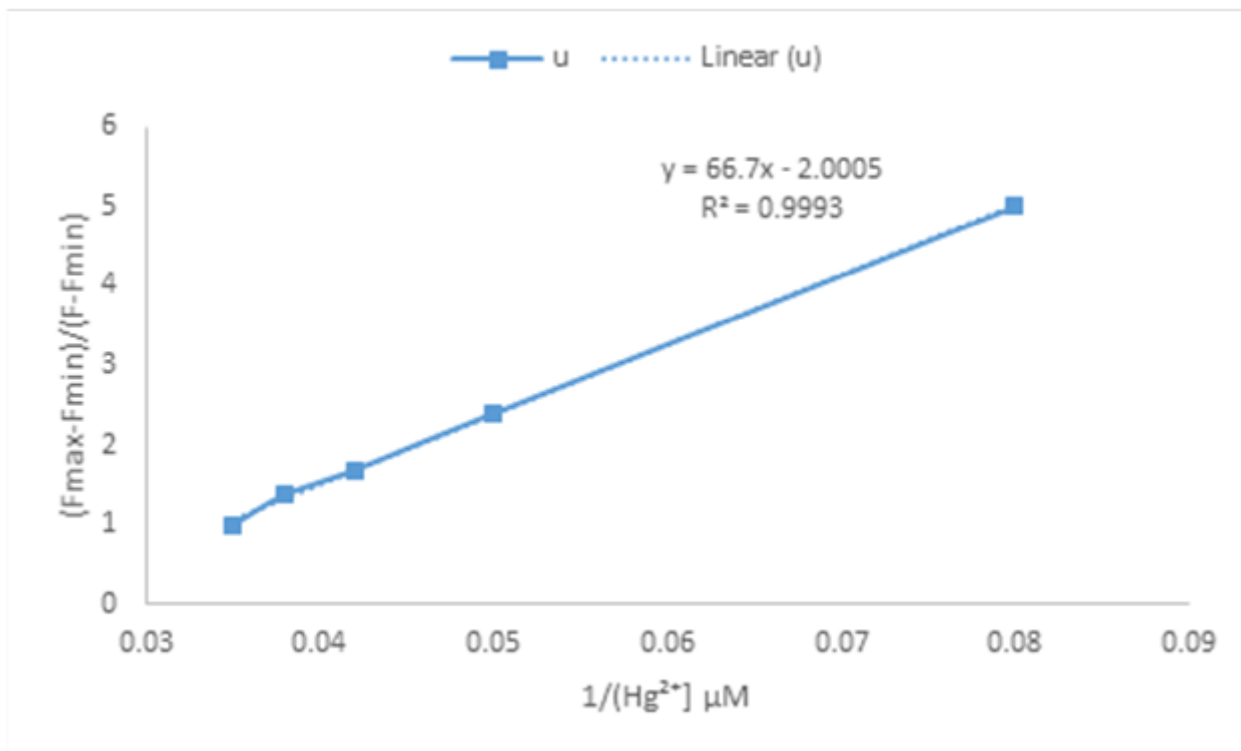


Figure 5

Benesi-Hildebrand plot of *(E)*-2-(2-aminophenylthio)-*N*-(thiophen-2-yl-methylene) benzenamine ( $1 \times 10^{-5}$  M) at different  $\text{Hg}^{2+}$  concentration

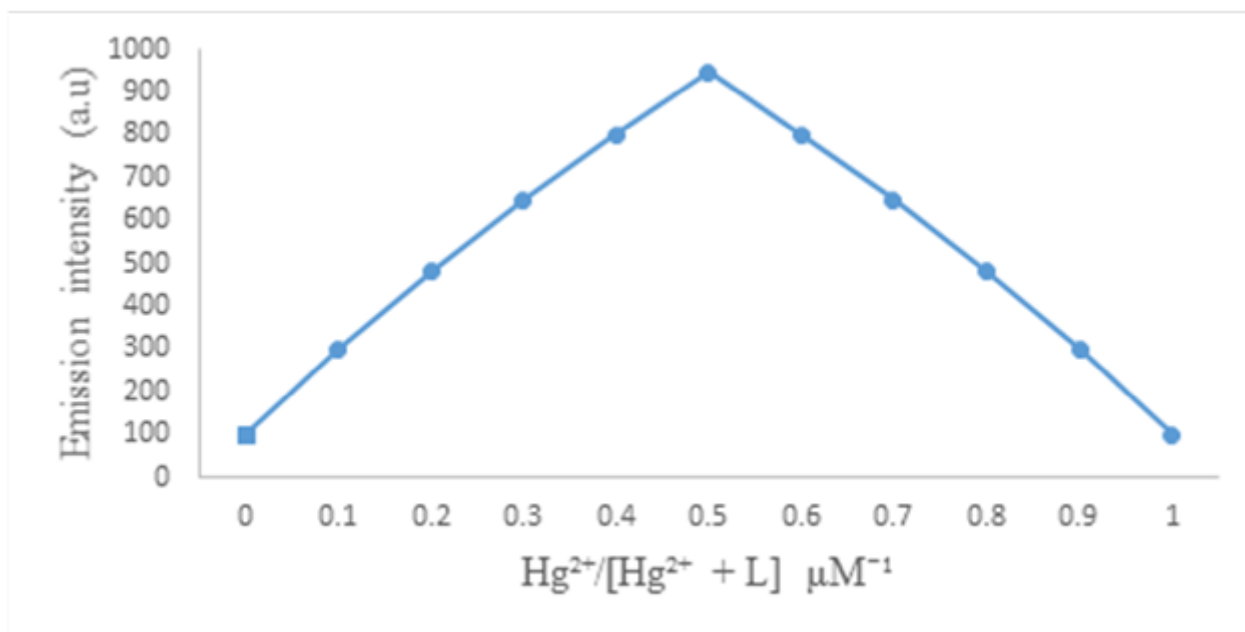
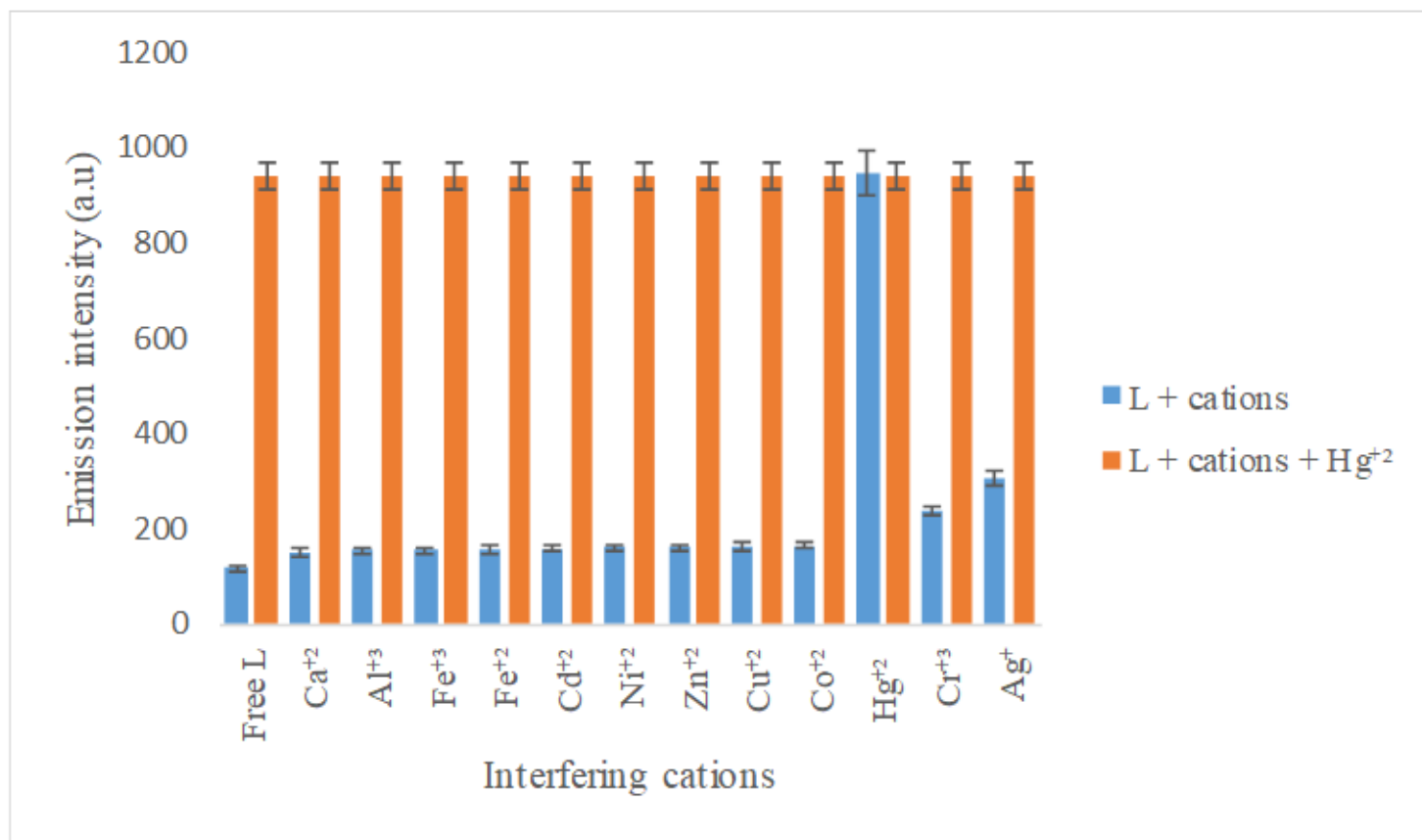


Figure 6



Job's plot of (*E*)-2-(2-aminophenylthio)-*N*-(thiophen-2-yl-methylene) benzeneamine with Hg<sup>2+</sup>



**Figure 7**

Competition experiment of (*E*)-2-(2-aminophenylthio)-*N*-(thiophen-2-yl-methylene) benzenamine selectivity toward Hg<sup>2+</sup> in the presence of metal other ions

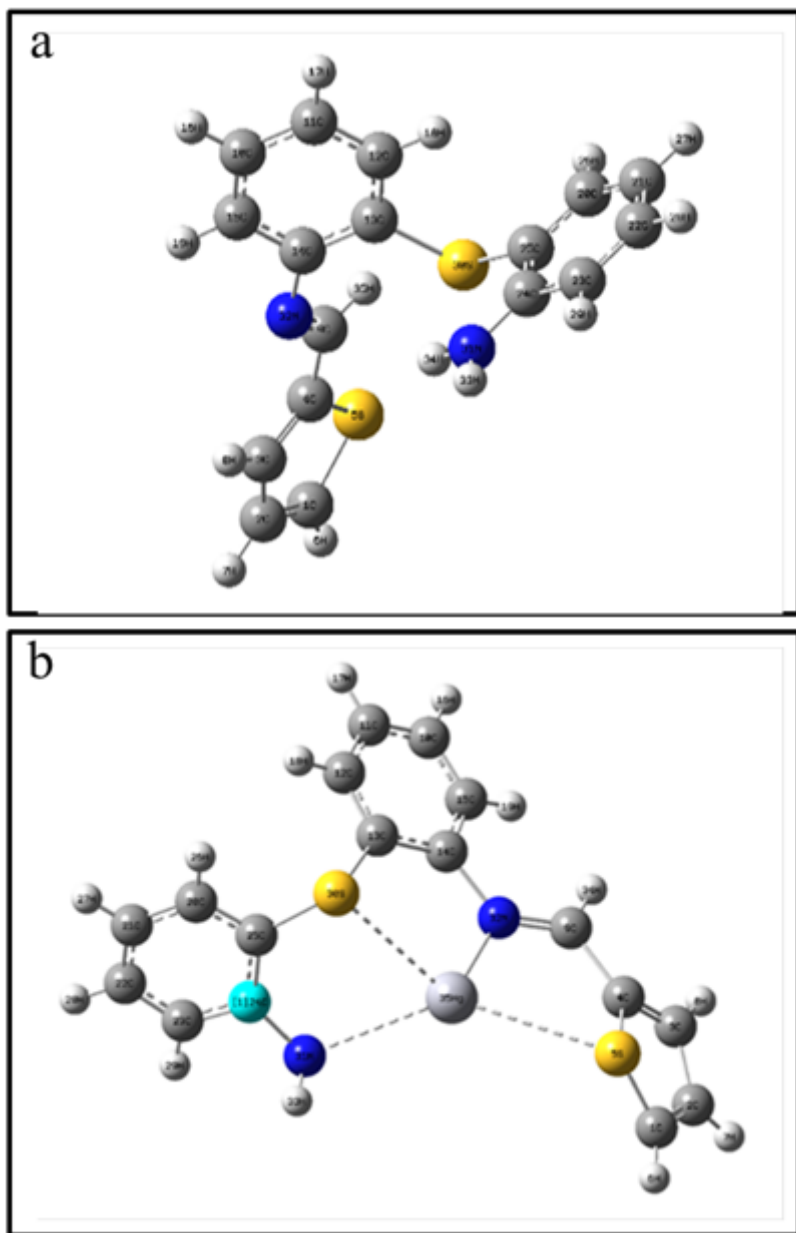


**Figure 8**

Optimized structure of the Schiff base and Schiff base-Hg complex

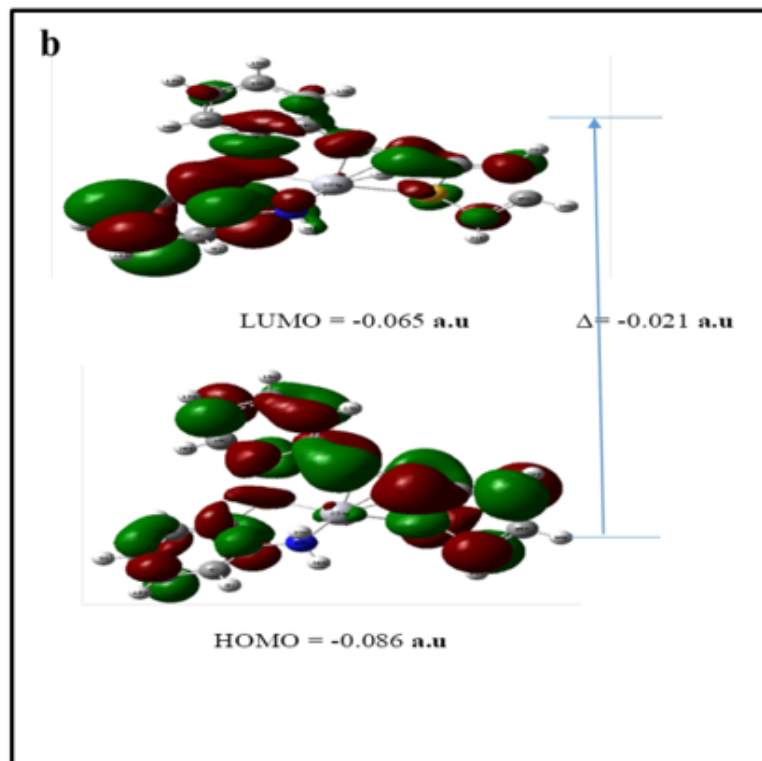
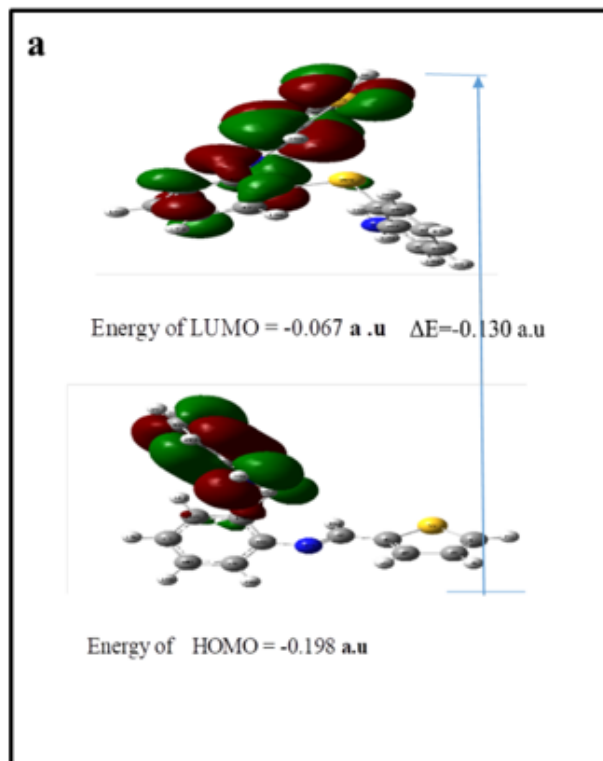


**Figure 9**

HOMO and LUMO energy diagram of the Schiff base and Schiff base-Hg complex

## Supplementary Files

This is a list of supplementary files associated with this preprint. Click to download.

- [Scheme1.png](#)
- [220930SupportingInformationV1AKM.docx](#)